Sensors and Actuators B 211 (2015) 42–51

Contents lists available at ScienceDirect

Sensors and Actuators B: Chemical

journal homepage: www.elsevier.com/locate/snb

A unified bottom up multiscale strategy to model gas sensors based on conductive polymers

M.S. Byshkin[a,d,*], F. Buonocore[b], A. Di Matteo[c,d], G. Milano[a,d,*]

[a] Modeling Lab for Nanostructure and Catalysis, Dipartimento di Chimica e Biologia and NANOMATES, University of Salerno, 84084, Via Ponte don Melillo, Fisciano, Salerno, Italy
[b] ENEA Casaccia Research Center, Via Anguillarese 301, 00123 Rome, Italy
[c] STMicroelectronics, Via Remo de Feo, 1, 80022 Arzano, Naples, Italy
[d] IMAST Scarl, Piazza Bovio 22, 80133 Naples, Italy

ARTICLE INFO

Article history:
Received 30 May 2014
Received in revised form
19 December 2014
Accepted 13 January 2015
Available online 20 January 2015

Keywords:
Gas sensors
Conducting polymers
Modeling
Response

ABSTRACT

A multiscale bottom up procedure, based on an atomistic description, able to model the sensing mechanism of devices based on intrinsic conductive polymers (ICP) is described. The proposed procedure has been successfully applied to describe the response of devices based on polyaniline (PANI), the most widely used material for this application. In particular, using a recently developed Monte Carlo technique, atomistic PANI structures at different doping levels have been modeled. Thermodynamic and conductivity properties obtained from atomistic simulations have been bridged to a macroscopic modeling scheme, describing diffusion and reaction processes and, finally, the time dependent sensor response in good agreement with experiments. A similar scheme has been then adopted in order to understand at molecular level the effect of humidity in the sensor response. The proposed approach is general and can be extended to different or more complex systems giving a useful connection between the microscopic structure of the sensing material and the sensor behavior.

1. Introduction

The electrical conductivity of intrinsically conducting polymers (ICP) is affected by exposure to various gases and it makes them useful for gas sensing application [1–4]. Sensors based on ICP are able to operate at room temperature, furthermore, ICP can be synthesized through easy chemical or electrochemical processes and modified conveniently by copolymerization or structural derivations [1–5]. On the other hand, micro- and nano-patterning of these sensing materials and formation of ultrathin sensing films facilitate enhanced vapor diffusion and response speed when compared to conventional polymeric films.

Doping and undoping processes play key roles in the sensing mechanism of ICP based sensors [5,6]. ICP can be doped by redox or protonation reactions. In the case of redox reaction some electrons are added or removed from ICP chains and charge carriers are formed. Differently, in the case of protonation reactions, the number of electrons does not change, but due to addition or removal of protons, the energy levels of ICP chains are rearranged. This doping type is observed in polyaniline (PANI) (see Fig. 1b). During the doping process conductivity of ICP can increase by up to 10 order of magnitudes. The conductivity may be also changed by modifying dopant type and material preparation method, however the effect of these structure modification is less strong and the resulting conductivity change of doped PANI is usually less than 2 orders of magnitudes [7,8]. Polyaniline in its forms (see Fig. 1) emeraldine base (PANI EB) or salt (PANI ES) are most widely used ICPs because of its ease of synthesis, high chemical and environmental stability and tunable properties [6,9–14].

Modeling the response of sensor to analyte gases at atomic level is particularly relevant to improve the development of devices [15]. Despite large interest in the potential applications of conducting polymer as gas sensors, a detailed molecular picture of the sensing mechanism of PANI (and more in general ICP) based devices is still under debate [5,6,16]. For example though importance of humidity in the PANI sensing mechanism [5], molecular understanding of response of PANI to humidity is not well established and several different mechanisms have been proposed: polymer swelling, increase in the interchain electron transfer and enhancement of dopant ions mobility [17,18]. Last but not least, there is no commonly accepted model for the charge transport in ICP [19].

* Corresponding authors at: Modeling Lab for Nanostructure and Catalysis, Dipartimento di Chimica e Biologia and NANOMATES, University of Salerno, 84084, Via Ponte don Melillo, Fisciano, Salerno, Italy. Tel.: +39 89 969567/9391.
E-mail addresses: mbyshkin@unisa.it (M.S. Byshkin), gmilano@unisa.it (G. Milano).

http://dx.doi.org/10.1016/j.snb.2015.01.039
0925-4005/

The steady state response is basically controlled by interaction of gas molecules with sensing material, while the time-dependent response depends also on transport of gas molecules inside sensing material. Several macroscopic phenomenological approaches have been used to model the time dependent response of sensors based on ICP. In particular, chemisorption and diffusion reaction models are usually used for modeling the time dependent response of conducting polymers. Chemisorption model [20] assumes that the sensing properties are completely defined by dynamics of surface adsorption and is proposed for very thin films. Diffusion reaction model [16] assumes that the guest molecules go quickly to the surface, but the limiting step for sensing is the diffusion of gaseous species into the polymer bulk. Although these approaches are very useful to understand the effects of macroscopic variables (film thickness, transport properties, material conductivity) they have several limitations. In particular, the large number of parameters needed to fit the model results to experimental sensor response makes a molecular interpretation of the behavior very difficult. For this reason, from this kind of modeling, clear indications about possible chemical or morphological alterations aimed to modify or improve the performances in a given direction are difficult to obtain. Furthermore, these approaches need several strong and sometimes oversimplifying assumptions on important aspects such as the behavior of electrical conductivity during the sensing experiments [16,20].

On the other hand, for a microscopic modeling, atomistic simulations are very useful for a detailed understanding of several phenomena and, in particular, for structure properties relationship of polymeric materials these studies have been performed since a long time [21,22]. However, these simulations usually limited on nanosecond and nanometer scales are not applicable to study processes involved in the sensor response occurring on macroscopic time (>s) and length scales (>μm). Therefore, in order to bridge this gap, computational schemes aimed to connect the microscopic and macroscopic descriptions in a bottom to up fashion would be very useful.

In this paper we propose a combination of molecular and finite element simulations to model PANI based gas sensor behavior starting from atomic structure and its modifications during the doping process. In particular, to model the microscopic scale, we propose a scheme based on combination of a recently developed Grand Canonical Monte Carlo technique (UEMC) [23] and the calculation of electrical conductivity from atomistic PANI structures at different doping levels. These results are casted in a diffusion reaction scheme giving a connection between microscopic structures and the response of ICP sensors to analyte gases.

The paper is organized as follows. The method for modeling the electrical conductivity of atomistic ICP structures is proposed in Section 2 and strategy for sensor response modeling is described in Section 3. In particular in Section 3.1 atomistic models of PANI and their electrical behavior are discussed. Finite element method (FEM) simulations of the sensor behaviors are presented in Section 3.2 (response to acidic gases) and analytical expressions for the sensor response to nonacidic gases are proposed in Section 3.3.

2. Methods and models

The electrical conductivity of ICP may be studied by atomistic simulation [24,25]. Once the atomistic structure is obtained, the conjugated segments (hopping sites) are defined, the parameters of Marcus equation [26] for charge hopping rate are estimated by different models and the time evolution of charge is modeled. Though the determination of conjugated segment is often empirical, the simulation of charge transport by these models is too time consuming to study the effect of doping level on ICP conductivity. Here we propose a more simple model, based on existing charge transport models. The existing models are: (1D) variable range hopping (VRH) with interchain coupling [27,28], 3D VRH [29,30], charging energy limited tunneling (CELT) model [31] and others. For detailed reviews see [7,32]. Usually these models suppose that there are conducting regions with insulating separation. The size of PANI conducting regions was estimated to have size 4.98 nm [32] and 8 nm [33] with separation distance 2.8 nm [32] and 1.6 nm [33]. Taking into account that size of PANI unit is about 2 nm (see Fig. 1b), we assume that doped PANI units may be considered as conjugated segment.

The details of atomistic simulation of PANI are given in supplementary material. Both the effect of doping level and the effect of structure modifications, e.g. swelling or chain conformations, on conductivity are included using this molecular description. The scheme proposed here is based on the description provided by the Miller–Abrahams equation, which is a popular charge transport model in disordered organic materials [34,35],

$$\omega = \varpi_0 \exp\left[-\frac{\Delta E}{kT}\right] \cdot \exp\left[-\frac{2s}{L}\right] \quad (1)$$

ω is the probability of charge transfer, s is the distance between two conductive units and L is the model parameter which is often called the localization length. When temperature T is constant we can assume that the temperature dependent term $\Delta E/kT$ is constant

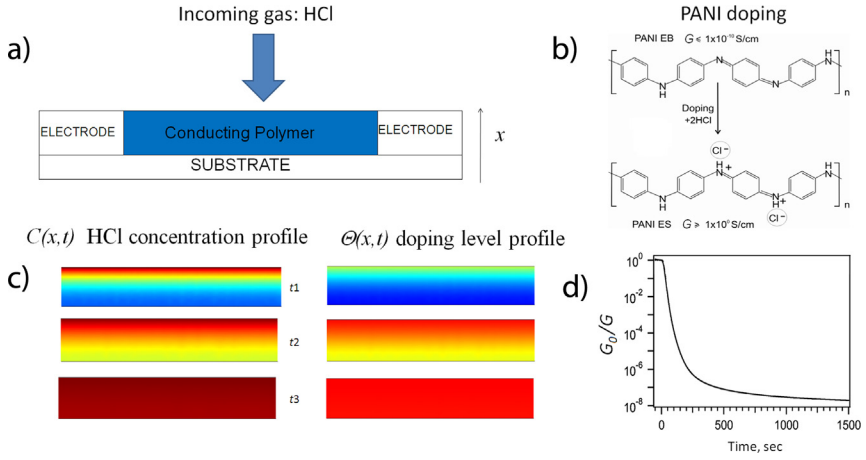

Fig. 1. Schematization of the working scheme of a sensing device. (a) PANI film exposed to an incoming gas, (b) PANI doping reaction with HCl leading to EB and ES forms, (c) gas concentration ($C(x,t)$) and doped level ($\Theta(x,t)$) density profiles, and (d) typical response of a sensing device.

and the hopping rate can be written as a function of the distance s between hopping centers,

$$\omega_{ij} = A \exp\left(-\frac{s_{ij}}{L}\right) \quad (2)$$

where A is a conductivity scaling constant.

Charge transfer processes can be modeled, for instance, using kinetic MC approaches [24,36]. Instead of modeling time evolution of charge transfer, we used Landauer formula to transfer the probabilities ω_{ij} of electron hopping between pairs of doped PANI units (2) to conductivities G_{ij} between these units [37]:

$$G_{ij} = \frac{2e^2}{h}\omega_{ij} \quad (3)$$

where $2e^2/h = 1/12.905\,\mathrm{k\Omega}$ is quantized conductivity. In this way each atomic configuration can be transformed into a nonregular network of sites, with resistance between sites given by Eqs. (2) and (3).

Releasing the periodic boundary conditions along one of axis, the conductivity of the resistor network between two opposite faces of simulation cell can be calculated by generalized transfer-matrix method introduced by one of us [38].

3. Results and discussion

As already mentioned, in the frame of the reaction–diffusion model, the analyte gas is supposed to go quickly to the surface and the limiting step for sensing is the diffusion into the polymer bulk. In this way, the effect of analyte gas on ICP sensor is basically controlled by several factors: transport, reactions of this gas with ICP and effect of interactions of gas with ICP on electrical conductivity. In particular, in Fig. 1a the sensing device is schematized. Qualitative concentration profiles are shown in Fig. 1c. In the case of PANI interacting with acidic gases like HCl a protonation reaction occurs (see Fig. 1b) transforming PANI-EB units (having low conductivities) into PANI-ES units (having much higher conductivities). For this reason, the concentration profile of HCl gives rise to a concentration profile of doped sites. The sensor response is then related to the local changes in the conductivity due to doping and its dynamical response is related to the rate of diffusion process. In Fig. 1d the typical time behavior of the reduced resistance (R/R_0) is reported. From the figure it is clear that the typical sensor response time exceeds the time that can be reached by atomistic simulations (order 100 ns). Furthermore, the order of magnitude of the film thickness is >μm well beyond the nm scale.

We propose a combination of atomistic and FEM simulations to model the sensor response and to give a detailed molecular description of the sensing process. The proposed approach is summarized in Scheme 1. In particular, in the four panels of this scheme the procedures together with the main equations are shown. The proposed approach can be divided in four main steps, two on the microscopic scale (steps 1 and 2 at the bottom of the scheme) and other two on the macroscopic scale (steps 3 and 4) on the top of Scheme 1. In the step 1, using a recently developed reactive UEMC scheme [23], it is possible to generate reliable atomistic models of partially doped structures having doping levels ranging from 0 (all polymer repeating units are PANI-EB) to 1 (all polymer repeating units are PANI-ES). These structures are used for step 2 (left panel on the bottom of Scheme 1, in which using molecular dynamics (MD) and traditional GCMC simulations diffusion coefficients and gas solubility are calculated. A further use of these structures is the calculation of local conductivity as a function of doping level (right panel on the bottom of Scheme 1), calculation of polymer conductivity $G(\theta)$ for different doping levels). As explained in a more detailed way later, this is a key ingredient of the proposed scheme. This important information together with gas concentration $C(x,t)$ and doping level $\Theta(x,t)$ profiles (left panel on the top of Scheme 1) are used to calculate the sensor conductivity as function of time i.e. sensor response. A first example application of the proposed scheme is the behavior of PANI based sensor for HCl detection and is considered in the following.

3.1. Modeling conducting polymer electrical conductivity

After the initial structure of fully doped PANI-HCl was generated, UEMC simulations have been used to generate atomic structures at different doping levels (see supplementary material). In particular, the value of dopant chemical potential μ was decreased step by step and the resulting doping levels are presented in Fig. 2 (filled symbols). By decreasing the chemical potential μ the doping level of PANI structure decreased until a totally undoped PANI EB was obtained. The typical structures obtained at three different values of doping level ($\Theta = 0.21$, 0.33 and 0.6) are shown in Fig. 2.

Using the proposed conductivity model, the electrical conductivity of obtained PANI structures was calculated. The obtained doping level dependence of specific conductivity is compared with experimental results in Fig. 3. Although the strong dependence of electrical conductivity on doping level is obviously the main factor making conducting PANI useful for chemical resistors, only few experimental studies were done [39–41]. The possible reason is the difficulty in the measurements of the doping level. The results from pioneering work of Macdiarmid [40] for HCl doped PANI are shown in Fig. 3 by empty squares. Much more recently more accurate measurements were performed and smoother dependences were obtained for picric acid doped PANI [39], shown by symbols empty triangles. The reported values of PANI-EB specific conductivity varies in wide range from 10^{-8} S/m to 10^{-5} S/m [8] and 10^{-4} S/m [42].

Neglecting the conductivity of PANI-EB, both experimental dependences presented in Fig. 3 can be well fitted by a percolation power law with the same exponent and threshold $\Theta_{th} = 0.204$,

$$G(\Theta) = a[\Theta - \Theta_{th}]^{3.8} \quad (4)$$

having different values of prefactor a (4×10^2 and 3.2×10^4 S/m for HCl and picric acid respectively). Calculated values (filled circles in Fig. 3) well agree with experiments. Hence it may be concluded that $G(\Theta)$ dependence for HCl and picric acid doped PANI differs by A conductivity scaling constant of Eq. (2) only. According to this behavior, the only parameter depending on the gas molecule is the prefactor A that is not necessary for the calculation of relative conductivity needed for sensor response. Calculated values of $G(\Theta)$ well agree in all range with the experimental points and with the analytic power law. According to the experimental results, a very fast increase of conductivity is observed for values of doping level around the percolation threshold ($\Theta \equiv 0{\cdot}204$). In fact, small increase of doping level from $\Theta = 0.21$ to $\Theta = 0.33$ corresponds to large increase of conductivity (more than four order of magnitudes). Significant, but less pronounced, increase can be obtained going from $\Theta = 0.33$ to $\Theta = 0.66$ (less than two order of magnitudes).

A microscopic picture of the percolation behavior in doped PANI structures can be obtained considering the tridimensional arrangement of regions showing higher conductivities as can be obtained from atomistic simulations. In particular, by making summation between all pairs of hopping sites the local conductivities as function of position $\hat{G}(x,y,z)$ can be defined as: $\hat{G} \equiv \sum_{i,j}(2e^2/h)\omega_{ij}$. Tridimensional structures can be visualized plotting isosurfaces of $\hat{G}(x,y,z) = 0.05 \cdot G_{PANI-HCL}$, where $G_{PANI-HCL}$ is the conductivity of fully HCl doped structures. In Fig. 3b these isosurfaces are reported for doping levels $\Theta = 0.21$, 0.33 and 0.6. From the figure it is clear that at $\Theta = 0.21$, several conductive regions are present but in confined regions. At $\Theta = 0.33$ the conductive regions are more extended

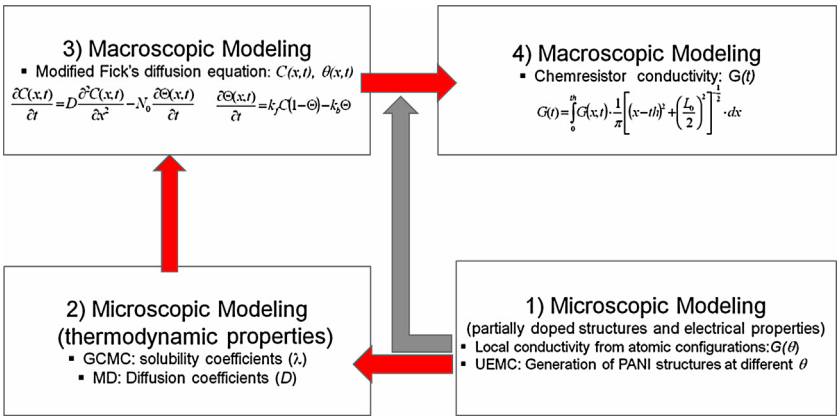

Scheme 1. Proposed bottom to up modeling approach. Four panels corresponding to the modeling steps and their mutual connections are depicted. On the bottom and on the top of the scheme the two microscopic and macroscopic steps are shown, respectively. (1) Microscopic modeling (generation of atomic structures) of the doping process by UEMC simulations and calculation of local conductivity from atomic configurations. (2) Microscopic modeling (calculation of thermodynamic properties) using atomic structures coming from step 1 by MD (diffusion coefficients) and CGMC (solubility). (3) Macroscopic modeling of the diffusion reaction process (modified Fick's equation) using solubility and diffusion coefficients coming from step 2. (4) Macroscopic modeling of sensor response $G(t)$ using $C(x,t)$ and $\Theta(x,t)$ coming from step 3 and conductivity $G(\theta)$ coming from step 1.

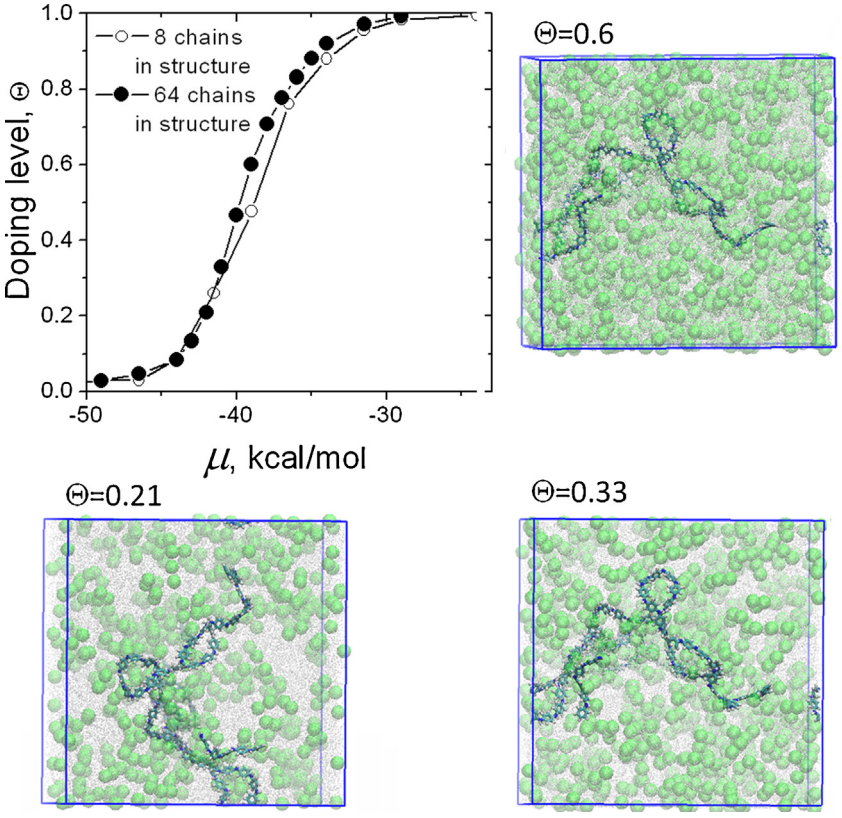

Fig. 2. Results of UEMC simulations (step 1, see Scheme 1). Calculated dependence of equilibrium doping level on HCl chemical potential. Using UEMC simulations it is possible to generate atomic structures of PANI-HCl at different doping levels from 0 to 1. Atomic structures corresponding to doping levels $\Theta = 0.21$, 0.33 and $\Theta = 0.6$ are shown. In the pictures for clarity reasons only one PANI chain is shown and chlorine atoms are highlighted using green spheres. The remaining atoms are depicted as gray points. (For interpretation of the references to color in this figure legend, the reader is referred to the web version of this article.)

and percolated regions appear, this feature becomes more pronounced at $\Theta = 0.6$.

Another remark of this section is the validation of the initial choice of a hopping site considering only double-doped units. With this choice of hopping site a good agreement of simulation and experiment is obtained with the value of localization length $L = 0.1$ nm, which can be compared with the value 0.6 nm [25], estimated using Efros–Shklovskii VRH model [22]. As showed by both *ab-initio* and classical simulations, doped PANI units can exist in two forms, with only one ($1N^+$) or both doped nitrogen atoms (see Fig. 1b) in partially doped PANI structures [23]. Our conductivity model gives agreement with experiment only if the $1N^+$ PANI units are not considered as conducting (hopping) centers (filled circles in Fig. 3). If they are considered conducting the threshold doping level Θ_c, obtained by simulation, decreases to almost zero and experimental results cannot be fitted by any realistic value of localization length L. For example, in Fig. 3 results of conductivity calculations performed using this assumption (reported as empty circles) show

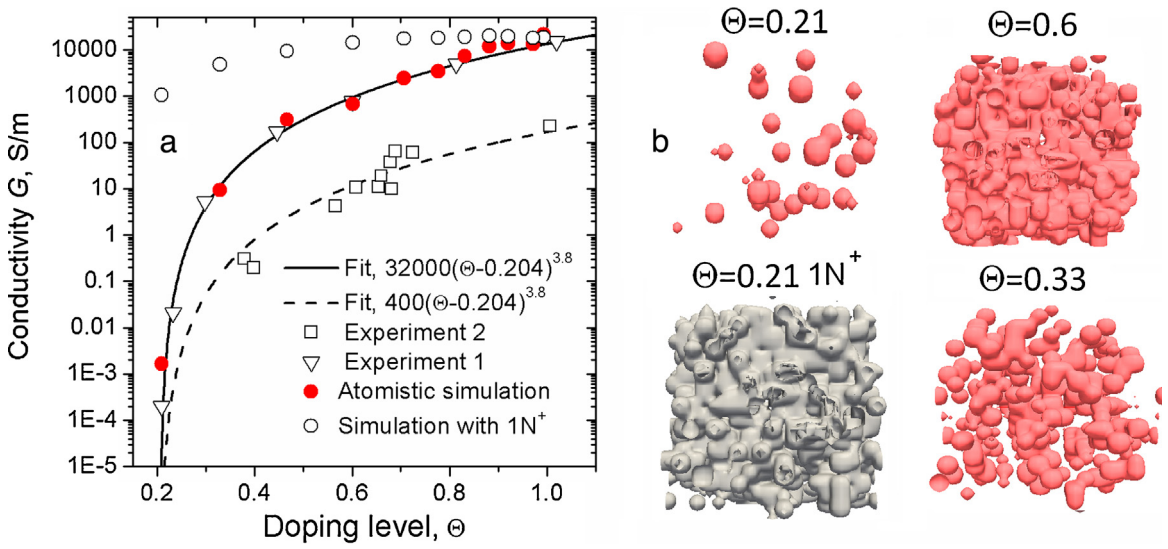

Fig. 3. (a) Doping level dependence of PANI electrical conductivity $G(\Theta)$: results of experiment 1 [39] and experiment 2 [40] are compared with the modeling results shown by red filled circles. If partially doped PANI units ($1N^+$) are considered as conducting the modeling (symbol ○) and the experimental results do not agree. (b) Local conductivity isosurfaces.

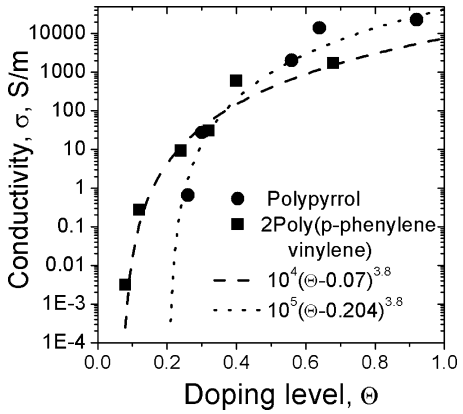

Fig. 4. Doping level dependence of conductivity of polypyrrole and poly(p-phenylene vinylene) at 300 K [43]. Lines are fits with (4) with Θ_{th} ¯ 0.204, $a = 10^5$ S/m and Θ_{th} ¯ 0.07, $A = 10^4$ S/cm, correspondingly.

that very large conductivity values can be obtained starting from very low values of Θ. It is interesting also to look in this case to the 3D structure of conducting region being percolated already at low doping levels (Fig. 3b).

The conductivity, doping level and density of states of PH_6 doped polypyrrole and $FeCl_3$ doped poly(p-phenylene vinylene) were studied in group of Mennon [43]. The reported doping level dependences of conductivity are shown in Fig. 4. Polypyrrol was considered fully doped when the monomer charge reaches 0.25 [43,44] and the doping level is defined as the charge per 4 monomers. It turns out that the percolational behavior (4) describes also the doping level dependence of conductivity of these two ICPs, with the same threshold $\Theta_{th} \equiv 0{\cdot}204$ for polypyrrole and smaller threshold $\Theta_{th} \equiv 0{\cdot}07$ for poly(p-phenylene vinylene).

3.2. Bridging atomistic to FEM simulations.

We consider gaseous acid species, e.g. HCl, (more in general *HX*), diffusing into a homogeneous PANI-EB film and reacting with it. The reaction is

$$PANI + HX \rightarrow PANIH^+X^- \tag{5}$$

Gardner et al. [16] proposed a modified Fick's diffusion equation to model the diffusion/reaction process of gas inside the polymer bulk. Assuming the planar geometry of the film, the following one-dimensional equation can be written for the gas diffusion:

$$\frac{\partial C(x,t)}{\partial t} = D\frac{\partial^2 C(x,t)}{\partial x^2} - N_0\frac{\partial \Theta(x,t)}{\partial t} \tag{6}$$

where C is the concentration of the gas, D is the diffusion coefficient, Θ is the doping level and N_0 is the density of reaction sites. It was supposed that all PANI reaction sites are equivalent and the probabilities of a reaction of *HX* with PANI reaction sites are the same:

$$\frac{\partial \Theta(x,t)}{\partial t} = k_f C(1-\Theta) - k_b\Theta \tag{7}$$

where k_b and k_f are the backward and forward rates of the reaction (5) respectively.

The typical chemresistor geometry is shown in the inset of Fig. 1a. With ICP film thickness *th* the initial and boundary conditions are the following $C(x,\ t=0)=0,\ 0\le x<th$; $C(x=th,\ t)=C_0$; $dC/dx=0,\ t=0,\ x=0$; $d\Theta/dx=0,\ t=0,\ \Theta=0$. Therefore, in order to solve Eqs. (6) and (7), the concentration of gas on the surface of PANI film C_0 is also required. The solution gives $C(x,\ t=\infty)=C_0$ and thus C_0 is given by the thermodynamic equilibrium. The Henry's law can be used for small concentration of gas $C_0=\lambda c$, where c is the concentration of gas vapor, supposed to be homogeneous in the environment out of the film, and λ is the solubility coefficient.

No closed analytical solutions can be found for Eqs. (6) and (7) when applied to transient signals. The values of diffusion coefficients D and solubility coefficient λ for HCl in PANI have been estimated by atomistic simulations (see supplementary material). The obtained values are $D = 3\times10^{-13}\ m^2/s$ and $\lambda = 7\times10^{-4}\ mol/m^3/ppm$. Nonetheless, once the D, k_b, k_f, N_0 and λ parameters are assigned, numerical solutions are calculated by the FEM. We have applied the finite element method (FEM) as implemented in the COMSOL Multiphysics software [45].

The conductivity G of a chemresistor with semi-infinite thin electrodes, thickness *th* and gap length L_0 is approximately given by [16]

$$G(t) = \int_0^{th} G(x,t)\cdot\frac{1}{\pi}\left[(x-th)^2 + \left(\frac{L_0}{2}\right)^2\right]^{-1/2}\cdot dx \tag{8}$$

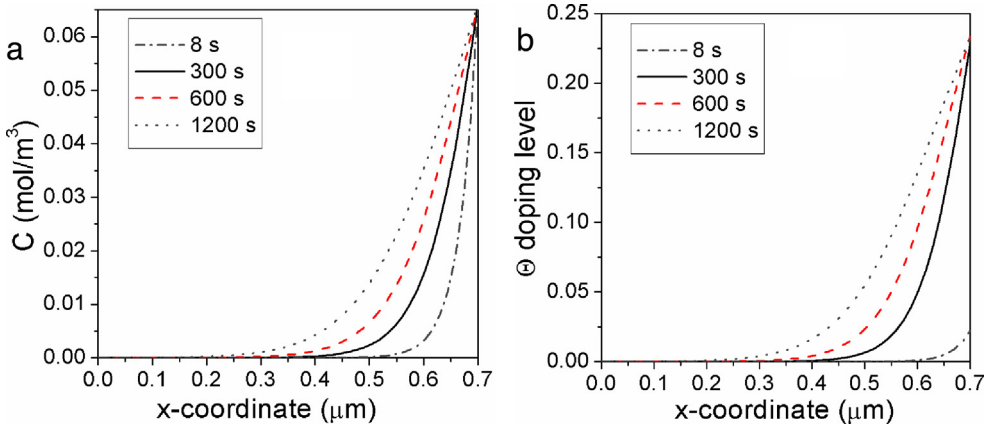

Fig. 5. Concentration $C(x,t)$ of HCl (a) and doping level $\Theta(x,t)$ (b) profiles calculated solving Eqs. (8) and (9) for PANI-EB films ($th = 0.7$ μm) exposed to 100 ppm HCl.

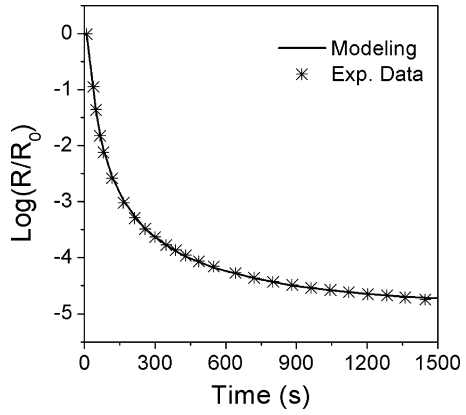

Fig. 6. Theoretical response of PANI-EB films to 100 ppm HCl for $k_f = 1.4 \times 10^{-2}$ m^3/mol/s, $k_b = 3.1 \times 10^{-3}$ s^{-1}, $D = 3 \times 10^{-13}$ m^2/s and $\lambda = 7 \times 10^{-4}$ mol/m^3/ppm compared to experimental data from [31].

Because the molecular mechanism by which conduction takes place in conducting polymers cannot be considered in FEM literature, it is usually assumed that $G(x, t)$ has a linear dependence on $\Theta(x,t)$ [15,16]. In our case we can use the more reliable behavior obtained from atomistic simulations, given by Eq. (4).

Virji et al. [46] studied the response of conventional and nanofiber PANI sensors to different gases. The sensors were fabricated by casting PANI films onto interdigitated electrode sensor substrate. The electrical dynamic response of sensor with conventional PANI-EB film to 100 ppm HCl was reported. We use Eqs. (4)–(8) to model the response and compare experimental and theoretical behaviors. By performing FEM simulation Eqs. (6) and (7) were solved and profiles of HCl concentration $C(x,t)$ and PANI doping level $\Theta(x,t)$ were obtained. They are presented in Fig. 5. The profiles result from the trade-off between the diffusion process and the reaction rate. In our case there is a significant number of reaction sites that adsorbs the diffusing gas and slows down the diffusion process. Using Eqs. (4) and (8) the response expressed as R/R_0 was obtained and is compared with the experimental results in Fig. 6. We assume the density of reaction sites in PANI as $N_0 = 7100$ mol/m^3 consistently with microscopic simulations data. The geometrical parameters of the chemresistor from reference [31] are the diffusive film thickness $th = 0.7$ μm and electrode distance $L_0 = 10$ μm. The nonzero conductivity of PANI EB was set to $G_{PANIEB} = 10^{-8}$ S/m [8]. The reaction rates describing the dynamics of reaction (5) are fitted as $k_f = 1.4 \times 10^{-2}$ m^3/mol/s and $k_b = 3.1 \times 10^{-3}$ s^{-1}.

3.3. Modeling the response to nonacidic gases

The interaction of water vapor with PANI, its role on PANI conductivity and in turn on sensor response is an important aspect still under debate [5]. Due to the ubiquity of water vapor in usual conditions of use of sensors a molecular understanding of this aspect is very important.

As shown in Fig. 2 atomistic simulation provides a relation between HCl chemical potential and PANI doping level $\Theta(\mu)$. In order to understand the effect of humidity on doping level the dependence of doping level on chemical potential $\Theta_H(\mu)$ was also obtained for PANI structure with adsorbed water [23]. It turns out that both dependences can be well described by cumulative distribution function of Gaussian distribution. Furthermore the humidity modifies this dependence so that $\Theta_H(\mu) = \Theta(\mu + E_{gas})$, where E_{gas} is the effect of adsorbed vapor. The value of E_{gas} is given by energy of interaction of PANI reaction sites with adsorbed gas molecules (see supplementary material for more details), and hence is proportional to the concentration of adsorbed gas C, $E_{gas} = e_{gas} \cdot C$. Thus the relation between PANI doping level and concentration of adsorbed vapor is obtained:

$$\Theta(C) = 0.5\left(1 + erf\left(\frac{\mu - B + e_{gas} \cdot C}{\sqrt{2\sigma^2}}\right)\right) \tag{9a}$$

With Henry's law $C = \lambda \cdot c$ we obtain

$$\Theta(c) = 0.5\left(1 + erf\left(\frac{\mu - B + e_{gas} \cdot \lambda \cdot c}{\sqrt{2\sigma^2}}\right)\right) \tag{9b}$$

where c is the concentration of analyte gas above gas sensor. Taking into account the strong dependence of polymers conductivity on doping level $\sigma(\Theta)$ and neglecting other possible effects of analyte gas on polymer conductivity, Eqs. (4) and (9b) may be used to model the steady state response of PANI to change of concentration c of analyte gas vapor. The values of σ and e_{gas} can be obtained by means of atomistic simulation (see supplementary material). We consider $\mu - B$ as a parameter that depends on many features such as polymer doping level, preparation method, dopant type, dissociation level, pH, etc.

Assuming that diffusion of analyte gas in ICP film may be described by Fick's law, the analytical expression for time-dependent sensor response can also be obtained. The Fick's diffusion in one dimension is given by the following equation

$$C(x, t) = C(x = 0) \cdot erfc\left(\frac{x}{2\sqrt{D \cdot t}}\right) \tag{10a}$$

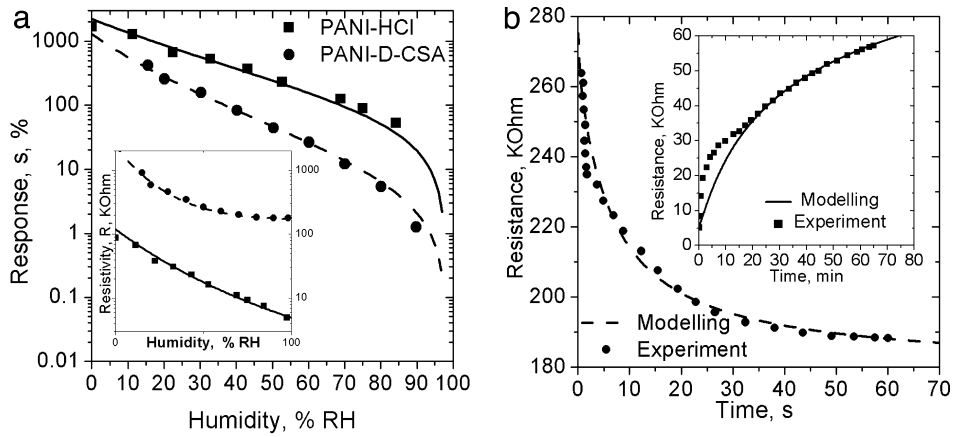

Fig. 7. (a) Experimental steady state responses of HCl and D-CSA doped PANI sensor [45,46] to humidity in comparison with modeling results (solid and dashed lines). The fitting parameter is $\mu - B = -1.4$ and $\mu - B = 1.1$ kcal/mol for PANI-HCl and PANI-D-CSA respectively. The corresponding chemresistor electrical resistivity is given in the inset. (b) Experimental time dependent PANI sensor responses in comparison with modeling results. The response of D-CSA doped PANI to change of RH from 45 to 90% [46] is in the main plot and the response of HCl doped PANI to change of RH from 98 to 0% [45] is given in the inset.

Substituting it to (9a) and using Henry's law $C(x=0) = \lambda \cdot c$, we obtain analytical expression for local doping level

$$\Theta(x,t) = 0.5\left(1 + erf\left(\frac{\mu - B + e_{gas} \cdot \lambda \cdot c \cdot erfc(x/2\sqrt{D \cdot t})}{\sqrt{2\sigma^2}}\right)\right) \quad (10b)$$

Substituting it to (4) and (8), the analytical expression for chemresistor conductivity G is obtained. Results are independent from the conductivity constant a if relative chemresistor resistance G_0/G or sensor response is calculated.

We use the experimental results of other research groups and show how these results can be modeled by Eqs. (4) and (9). The most recent papers where the responses of PANI sensor to humidity are reported in [47,48]. HCl doped PANI was fabricated directly onto the screen-printed electrodes using chemical deposition method [47]. Camphorsulfonic acid (D-CSA) doped PANI was prepared on interdigitated transducers by self-assembly process with different number of layers [48]. The response to humidity was defined as

$$s(RH) = \frac{R_{RH} - R_{98\%}}{R_{98\%}} \cdot 100\% \quad (11)$$

where R_{RH} is the sensor resistance at relative humidity RH. The reported experimental responses s and resistivity R_{RH} of PANI-HCl and PANI-D-CSA are given in Fig. 7a.

We now use Eq. (9b) to model the response of PANI to humidity. The values of $e_{gas} = 0.5$ and $\sigma = 4.4$ kcal/mol are obtained from results of atomistic simulation (see supplementary material), and solubility $\lambda = C_{100}/100\%$, where C_{100} is mass fraction of water adsorbed at relative humidity $RH = 100\%$. In the experimental work of Ostwal et al. [49] it was shown that the C_{100} is about 5% for PANIEB and 10% for fully doped PANI-HCl. Thus only the value of $\mu - B$ is unknown and is fitted to experimental result. Using Eq. (4) for $R^{-1}(\Theta)$ and (9b) for $\Theta(RH)$ the response $s(RH)$ of PANI-HCl is obtained and is shown in Fig. 7a by solid line. For simplicity we used $C_{100}(\Theta) = 5\%$ for all doping levels, however even the use of constant C_{100} value gives excellent results: by fitting the only parameter value $\mu - B$ a good agreement of theory with experiment is obtained.

The response of D-CSA doped PANI (Fig. 7a) is somewhat different. Indeed the strength of binding between dopant and PANI and the effect of water on this strength depend on type of dopant. The solubility of water in PANI depends on type of dopant too [49]. As UEMC study of D-CSA doped PANI was not performed,

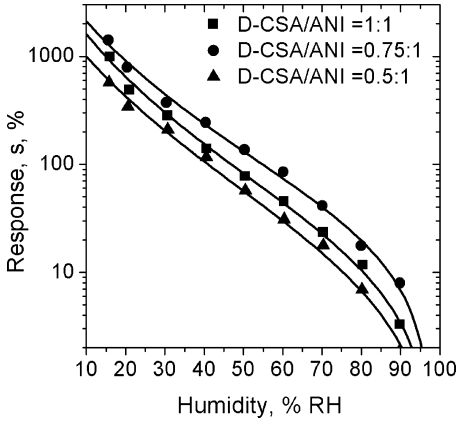

Fig. 8. Experimental steady state response (filled symbols) of 2-layer D-CSA doped PANI to humidity [46] in comparison with modeling results (solid lines). The fitted values of $\mu - B$ and $e_{gas} \cdot C_{100}$ are −0.4,17.5; −0.2, 21 and 0.3,22 kcal/mol for PANI sensors fabricated at D-CSA/aniline molar fraction 1:1; 0.75:1 and 0.5:1 respectively.

the estimation of $e_{gas} \cdot C_{100}$ value for this system was not done and we considered this value as another free parameter to fit the experimental response. It turns out that a good agreement between theoretical and experimental humidity responses of D-CSA doped PANI is obtained with the value $e_{gas} \cdot C_{100} = 16$ kcal/mol, 4 times higher than that for PANI-HCl. Higher $e_{gas} \cdot C_{100}$ value can be explained by either higher water solubility in D-CSA doped PANI or by stronger effect of water on equilibrium constant of protonation reaction. In inset of Fig. 7a the resistance values are also reported and compared with results obtained by Eqs. (4) and (9b).

More details concerning the sensors fabrications can be found in [47,48]. The PANI-D-CSA responses presented in Fig. 7 correspond to 6 layer PANI film prepared by self-assembly in solution of aniline and D-CSA with molar fraction 1:1. However different responses to humidity of sensors with thinner 2-layer PANI films fabricated at different solution of PANI and D-CSA were also reported in [48]. In Fig. 8 we compare reported experimental results (filled symbols) with modeling results (solid lines). One can see that all the responses to water are well described by proposed equations.

The experimental time-dependent response of PANI to change of humidity was also reported in papers [47,48] and is shown in Fig. 7b. It is possible to check if the time-dependent response can be modeled by Fick's diffusion using Eq. (10). The results obtained by Eqs. (4), (8) and (10b) are presented in Fig. 7b. All the

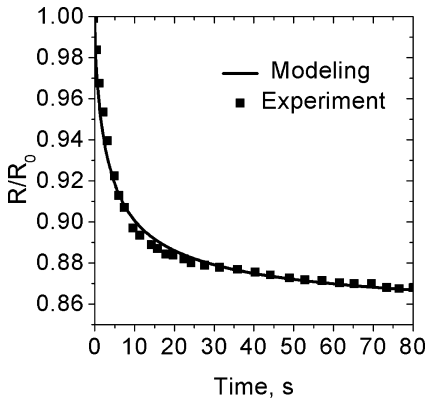

Fig. 9. Experimental time dependent response of PANI sensor to methanol [44] in comparison with the modeling results given by Eqs. (4) and (8)–(10). The fitted parameters are $e_{gas} \cdot C_{100} = 0.48$ and $\mu - B = -1.4$ Kcal/mol and diffusion coefficient $D = 4 \times 10^{-15}$ m^2/s.

values of parameters $\mu - B$, e_{gas}, σ, and C_{100} are those already used for the steady state response $R(RH)$, shown in Fig. 7a. The value of coefficient D of water diffusion in PANI is 3×10^{-13} m^2/s [49]. The values of electrode gap distance L_0 were reported as 20 μm [48] and 125 μm [47], but the thickness of PANI films *th* was not reported unfortunately and we had to fit its value. The fitted values of film thickness are 4.5 μm and 17 μm correspondingly, and are close to typical PANI sensor film thickness. We can see that though the Fick's diffusion can be used to model the time-dependent response to humidity, a visible difference between experiment and modeling is observed at small time. This difference may be easily explained. Indeed the transport of gas molecules in thin subsurface layer of PANI film is given by gas sorption kinetics and is not limited by diffusion. The roughness of the film surface can increase the thickness of the layer where the response is fast. At larger time however the gas transport is moderated by diffusion and good agreement of modeling with experiment is observed.

We finally show that proposed methodology can be used to model response of different ICPs to different gases. In the experimental work of Virji et al. [46] response of PANI sensor to 20,000 ppm methanol is reported. This response was explained by chain conformational changes. The approach we have proposed, that includes atomistic simulation, can be used to model the effect of analyte gas on both doping level, chain conformations and swelling, but performing the atomistic study is time consuming. Instead we evidence that the reported response of PANI to methanol can be well fitted by the same analytical equation that was used to model the response to humidity. This is shown in Fig. 9 where the reduced resistivity (filled symbols) from reference [46] is compared with modeling results (solid line). The reported sensor diffusive film thickness and electrode distance are $th = 0.3$ μm and $L_0 = 10$ μm, respectively.

It was reported that Cl^--doped polypyrrole increase the doping level and electrical conductivity under exposure to such gases as benzene, toluene, ethylbenzene, and xylene (BTEX) compounds [50]. The polypyrrol sensor was prepared by deposition of interdigitated screen-printed gold electrode with polypyrrole thin film. The reported sensor resistance changes [50] due to exposure to o-xylen and ethylbenzene vapors are shown in Fig. 10 by symbols. Using the doping level dependence of polypyrrole conductivity $\sigma(\Theta)$ shown in Fig. 4 together with (9b) we have function that can fit the reported experimental responses. The fitted results are shown in Fig. 10a by lines. The reported resistance change was not normalized and we had to consider conductivity normalization constant A as unknown parameter depending on sensor geometry. The fitted parameters $A = 5 \times 10^{-4}$ Ohm^{-1} and $\mu - B = 2$ kcal/mol characterize the sensor

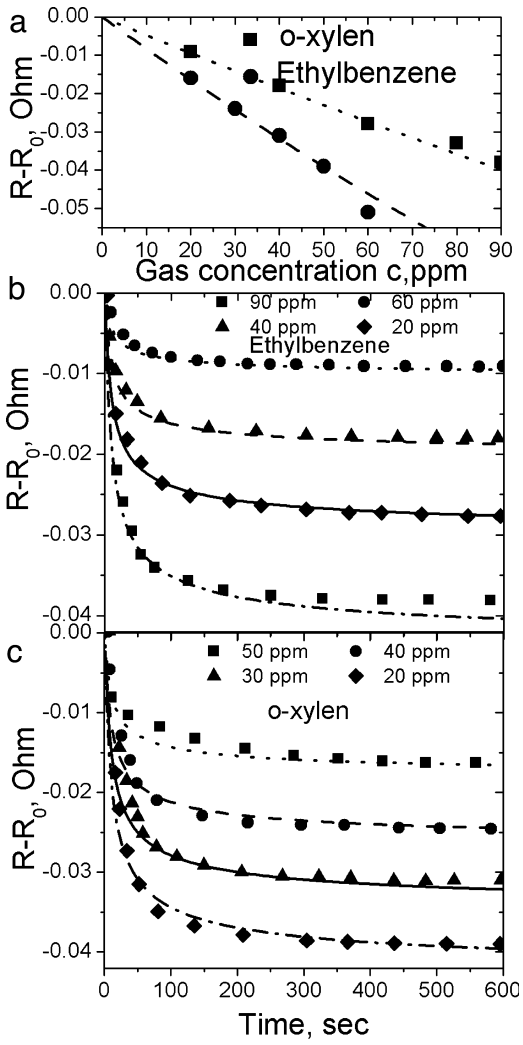

Fig. 10. The resistance change of polypyrrol sensor due to exposure to ethylbenzene and o-xylene vapors. The steady state response (a) and time dependent response (b,c). The symbols are results of experiment [50] and lines are results of proposed analytical equations with corresponding concentration c of gas vapor.

and should not depend on type of analyte gas, and the response to different gases can be obtained by varying $e_{gas} \cdot \lambda$ constant only. The obtained values of $e_{gas} \cdot \lambda$ are 0.0037 kcal/mol/ppm for o-xylene and 0.002 kcal/mol/ppm for ethylbenzene. The higher sensitivity to o-xylene is explained by higher solubility constant λ of o-xylene. The constant λ of solubility of gases in polymer increase with gas boiling temperature [50,51].

The obtained parameters are then used to model time dependent response using (4), (8) and (10b). The sensor parameters *th* and L_0 were not reported and we have 2 fitting parameters: L/th and D/th^2. It turns out that Eqs. (4), (8) and (10b) well describe the time dependent responses to vapors of both o-xylene and ethylbenzene with different vapor concentration c (solid lines in Fig. 10b and c). The same parameter values $L_0/th = 0.23$ and $D/th^2 = 0.031$ s^{-1} were used for all the time-dependent responses, shown in Fig. 10.

4. Conclusions

In this manuscript using a bottom to up modeling approach we described the sensing mechanism of PANI based sensor devices at atomic level of details. In particular, using a recently developed Monte Carlo technique we modeled PANI structures at different doping levels ranging from that of PANI EB to that of fully doped

PANI ES. Using an empirical model for the calculation of electrical conductivity of these structures a very good agreement with experimental data has been obtained. Thermodynamic and conductivity data obtained from atomistic simulations have been used in a macroscopic modeling scheme describing diffusion and reaction processes and finally the time dependent sensor response giving a good agreement with experimental data. The same scheme has been then adopted in order to understand the effect of humidity in the sensor response. According to Monte Carlo simulation results, we followed the hypothesis, that for a given value of gas chemical potential, the main effect of water molecules in PANI structures is to enhance the doping level with respect to dry structures. An analytical expression for the calculation of steady state and dynamic responses of the sensor to analyte gas has been proposed. The steady state response of PANI to humidity obtained by this expression agrees well with the experimental results. The dynamic response of PANI sensor to the change of relative humidity, obtained by this expression, agrees well with experimental results at all time, excluding small time values, where some deviations are observed and discussed.

The proposed simulation approach, able to describe at atomic level the sensing experiment, provides a molecular interpretation of the sensing mechanism in PANI based sensors. According to the simulation results, the main feature characterizing the sensing mechanism is the behavior of the doping level as function of the chemical potential. Using an accurate calculation of this behavior, it has been possible to accurately reproduce conductivity behavior and sensor response. Another important aspect is the correct reproduction of the effect of relative humidity on steady state and dynamic response of the sensor. It is worth noting that the proposed model gives a good reproduction in all range of relative humidity reported for experiments involving detection of HCl and D-CSA acids (for *RH* going from 0 to about 90%) assuming the same dependency of conductivity $G(\theta)$ of Eq. (4) obtained for systems without water molecules. This indicates that the main effect of water in the sensing mechanism is the enhancement of doping level due to stabilization of protonated sites.

Finally it has been shown that responses of polypyrrole sensor to ethylbenzene and o-xylene, reported in literature, are also well described by the proposed model. These results suggest that the proposed scheme, that can be extended with suitable modifications also to other sensing materials, would allow to understand the basic physic-chemical underlying mechanisms of sensing and to address possible materials modifications and improvements.

Acknowledgements

This study was supported by IMPRESA (Impiego di materiali polimerici compositi per la Realizzazione di Sensori integrati in dispositivi a basso costo in Applicazioni multisensoriali) Project DM60704 of the MIUR Italy

Appendix A. Supplementary data

Supplementary data associated with this article can be found, in the online version, at http://dx.doi.org/10.1016/j.snb.2015.01.039.

References

[1] N.E. Agbor, M.C. Petty, A.P. Monkman, Polyaniline thin films for gas sensing, Sens. Actuators B: Chem. 28 (1995) 173–179.
[2] M.M. Ayad, N.A. Salahuddin, M.O. Alghaysh, R.M. Issa, Phosphoric acid and pH sensors based on polyaniline films, Curr. Appl. Phys. 10 (2010) 235–240.
[3] J. Huang, S. Virji, B.H. Weiller, R.B. Kaner, Nanostructured polyaniline sensors, Chemi. – A Eur. J. 10 (2004) 1314–1319.
[4] J. Janata, M. Josowicz, Conducting polymers in electronic chemical sensors, Nat. Mater. 2 (2003) 19–24.
[5] H. Bai, G. Shi, Gas sensors based on conducting polymers, Sensors 7 (2007) 267–307.
[6] A.G. MacDiarmid, Synthetic metals: a novel role for organic polymers (nobel lecture), Angew. Chem. Int. Ed. 40 (2001) 2581–2590.
[7] S. Bhadra, D. Khastgir, N.K. Singha, J.H. Lee, Progress in preparation, processing and applications of polyaniline, Prog. Polym. Sci. 34 (2009) 783–810.
[8] J. Stejskal, D. Hlavatá, P. Holler, M. Trchová, J. Prokeš, I. Sapurina, Polyaniline prepared in the presence of various acids: a conductivity study, Polym. Int. 53 (2004) 294–300.
[9] L. Al-Mashat, K. Shin, K. Kalantar-zadeh, J.D. Plessis, S.H. Han, R.W. Kojima, et al., Graphene/polyaniline nanocomposite for hydrogen sensing, J. Phys. Chem. C 114 (2010) 16168–16173.
[10] S. Chen, G. Sun, High sensitivity ammonia sensor using a hierarchical polyaniline/poly(ethylene-co-glycidyl methacrylate) nanofibrous composite membrane, ACS Appl. Mater. Interfaces 5 (2013) 6473–6477.
[11] C. Ge, K.S. Orosz, N.R. Armstrong, S.S. Saavedra, Poly(aniline) nanowires in sol–gel coated ITO: a pH-responsive substrate for planar supported lipid bilayers, ACS Appl. Mater. Interfaces 3 (2011) 2677–2685.
[12] J. Gong, Y. Li, Z. Hu, Z. Zhou, Y. Deng, Ultrasensitive NH_3 gas sensor from polyaniline nanograin enchased TiO_2 fibers, J. Phys. Chem. C 114 (2010) 9970–9974.
[13] J. Wu, L. Yin, Platinum nanoparticle modified polyaniline-functionalized boron nitride nanotubes for amperometric glucose enzyme biosensor, ACS Appl. Mater. Interfaces 3 (2011) 4354–4362.
[14] W.-S. Huang, B.D. Humphrey, A.G. MacDiarmid, Polyaniline, a novel conducting polymer. Morphology and chemistry of its oxidation and reduction in aqueous electrolytes, J. Chem. Soc. Faraday Trans. 1 82 (1986) 2385–2400.
[15] Z.-F. Li, F.D. Blum, M.F. Bertino, C.-S. Kim, Understanding the response of nanostructured polyaniline gas sensors, Sens. Actuators B: Chem. 183 (2013) 419–427.
[16] J.W. Gardner, P.N. Bartlett, K.F.E. Pratt, Modelling of gas-sensitive conducting polymer devices, IEE Proc. – Circuits Devices Syst. (1995) 321–333.
[17] A.T. Ramaprasad, V. Rao, Chitin–polyaniline blend as humidity sensor, Sens. Actuators B: Chem. 148 (2010) 117–125.
[18] H.-X. Yin, M.-M. Li, H. Yang, Y.-Z. Long, X. Sun, Electrical resistance response of polyaniline films to water, ethanol, and nitric acid solution, Chin. Phys. B 19 (2010) 088105.
[19] R. Noriega, J. Rivnay, K. Vandewal, F.P.V. Koch, N. Stingelin, P. Smith, et al., A general relationship between disorder, aggregation and charge transport in conjugated polymers, Nat. Mater. 12 (2013) 1038–1044.
[20] H. Hu, M. Trejo, M.E. Nicho, J.M. Saniger, A. García-Valenzuela, Adsorption kinetics of optochemical NH_3 gas sensing with semiconductor polyaniline films, Sens. Actuators B: Chem. 82 (2002) 14–23.
[21] K.F. Mansfield, D.N. Theodorou, Atomistic simulation of a glassy polymer surface, Macromolecules 23 (1990) 4430–4445.
[22] F. Müller-Plathe, Local structure and dynamics in solvent-swollen polymers, Macromolecules 29 (1996) 4782–4791.
[23] M.S. Byshkin, A. Correa, F. Buonocore, A. Di Matteo, G. Milano, A united event grand canonical Monte Carlo study of partially doped polyaniline, J. Chem. Phys. 139 (2013) 244906.
[24] G. Ganzenmüller, T. Koslowski, Electronic conductivity in polyaromatic hydrocarbon glasses: a theoretical perspective, J. Chem. Phys. 125 (2006) 014707.
[25] V. Rühle, A. Lukyanov, F. May, M. Schrader, T. Vehoff, J. Kirkpatrick, et al., Microscopic simulations of charge transport in disordered organic semiconductors, J. Chem. Theory Comput. 7 (2011) 3335–3345.
[26] R.A. Marcus, Electron transfer reactions in chemistry. Theory and experiment, Rev. Modern Phys. 65 (1993) 599–610.
[27] J. Joo, S.M. Long, J.P. Pouget, E.J. Oh, A.G. MacDiarmid, A.J. Epstein, Charge transport of the mesoscopic metallic state in partially crystalline polyanilines, Phys. Rev. B 57 (1998) 9567–9580.
[28] Z.H. Wang, E.M. Scherr, A.G. MacDiarmid, A.J. Epstein, Transport and EPR studies of polyaniline: a quasi-one-dimensional conductor with three-dimensional "metallic" states, Phys. Rev. B 45 (1992) 4190–4202.
[29] A.L. Efros, B.I. Shklovskii, Coulomb gap and low temperature conductivity of disordered systems, J. Phys. C: Solid State Phys. 8 (1975) L49.
[30] Q. Li, L. Cruz, P. Phillips, Granular-rod model for electronic conduction in polyaniline, Phys. Rev. B 47 (1993) 1840–1845.
[31] P. Sheng, B. Abeles, Y. Arie, Hopping conductivity in granular metals, Phys. Rev. Lett. 31 (1973) 44–47.
[32] Y.-F. Lin, C.-H. Chen, W.-J. Xie, S.-H. Yang, C.-S. Hsu, M.-T. Lin, et al., Nano approach investigation of the conduction mechanism in polyaniline nanofibers, ACS Nano 5 (2011) 1541–1548.
[33] R. Pelster, G. Nimtz, B. Wessling, Fully protonated polyaniline: hopping transport on a mesoscopic scale, Phys. Rev. B 49 (1994) 12718–12723.
[34] N. Tessler, Y. Preezant, N. Rappaport, Y. Roichman, Charge transport in disordered organic materials and its relevance to thin-film devices: a tutorial review, Adv. Mater. 21 (2009) 2741–2761.
[35] L. Zuppiroli, M.N. Bussac, S. Paschen, O. Chauvet, L. Forro, Hopping in disordered conducting polymers, Phys. Rev. B 50 (1994) 5196–5203.
[36] M. Casalegno, G. Raos, R. Po, Methodological assessment of kinetic Monte Carlo simulations of organic photovoltaic devices: the treatment of electrostatic interactions, J. Chem. Phys. 132 (2010) 094705.
[37] W.S. Bao, S.A. Meguid, Z.H. Zhu, M.J. Meguid, Modeling electrical conductivities of nanocomposites with aligned carbon nanotubes, Nanotechnology 22 (2011) 485704.
[38] M.S. Byshkin, A.A. Turkin, A new method for the calculation of the conductivity of inhomogeneous systems, J. Phys. A: Math. Gen. 38 (2005) 5057.

[39] S.M. Ahmed, Preparation and degradation of highly conducting polyaniline doped with picric acid, Eur. Polym. J. 38 (2002) 1151–1158.
[40] A.G. Macdiarmid, J.C. Chiang, A.F. Richter, A.J. Epstein, Polyaniline: a new concept in conducting polymers, Synth. Met. 18 (1987) 285–290.
[41] P. Kiattibutr, L. Tarachiwin, L. Ruangchuay, A. Sirivat, J. Schwank, Electrical conductivity responses of polyaniline films to SO_2–N_2 mixtures: effect of dopant type and doping level, React. Funct. Polym. 53 (2002) 29–37.
[42] N.P. Chauhan, R. Ameta, R. Ameta, S.C. Ameta, Thermal and conducting behaviour of emeraldine base (EB) form of polyaniline (PANI), Indian J. Chem. Technol. 18 (2011) 118–122.
[43] I.N. Hulea, H.B. Brom, A.K. Mukherjee, R. Menon, Doping, density of states and conductivity in polypyrrole and poly(p-phenylene vinylene), Phys. Rev. B 72 (2005) 054208.
[44] H.C.F. Martens, H.B. Brom, R. Menon, Metal-insulator transition in PF6 doped polypyrrole: failure of disorder-only models, Phys. Rev. B 64 (2001) 201102.
[45] COMSOL Multiphysics 4.3a, www.comsol.com
[46] S. Virji, J. Huang, R.B. Kaner, B.H. Weiller, Polyaniline nanofiber gas sensors: examination of response mechanisms, Nano Lett. 4 (2004) 491–496.
[47] F.-W. Zeng, X.-X. Liu, D. Diamond, K.T. Lau, Humidity sensors based on polyaniline nanofibres, Sens. Actuators B: Chem. 143 (2010) 530–534.
[48] Z. Wu, X. Chen, S. Zhu, Y. Yao, H. Guo, Effect of humidity on electrical properties of micro/nano-polyaniline thin films with different D-CSA doping degree, Measurement 46 (2013) 411–419.
[49] M.M. Ostwal, B. Qi, J. Pellegrino, A.G. Fadeev, I.D. Norris, T.T. Tsotsis, et al., Water sorption of acid-doped polyaniline powders and hollow fibers: equilibrium and kinetic response, Ind. Eng. Chem. Res. 45 (2006) 6021–6031.
[50] C.W. Lin, Y.L. Liu, R. Thangamuthu, Investigation of the relationship between surface thermodynamics of the chemically synthesized polypyrrole films and their gas-sensing responses to BTEX compounds, Sens. Actuators B 94 (2003) 36–45.
[51] M.-J. Chang, Y.-H. Liao, A.S. Myerson, T.K. Kwei, Gas transport properties of polyaniline membranes, J. Appl. Polym. Sci. 62 (1996) 1427–1436.

Biographies

Maksym Byshkin is currently a post-doc in the Department of Chemistry and Biology, University of Salerno. Received M. Degree in mathematics in 2002 and Ph.D. in theoretical physics in 2008 at Kharkov Institute of Physics and Technology, Ukraine. Research interests include modeling of nanoparticles, polymers and composite materials and developing of modeling methods.

Francesco Buonocore received the M. Degree in physics in 1997 and the Ph.D. in 2001 from the University of Naples "Federico II". He had been an advanced research engineer in STMicroelectronics since 2001 until 2012. He is currently a researcher at ENEA and a visiting researcher at Oak Ridge National Laboratory. His research interests include the development of gas sensors and functional materials.

Andrea Di Matteo works in STMicroelectronics from July 2004. His current position is the R&D Manager. He got his degree in chemistry in 1995 and a Ph.D. in theoretical chemistry. His scientific formation has been further improved at the Ecole Normale Superiore de Paris (ENS), University of Padova and the Centre Energie Atomique, CEA Grenoble France. His main research interests include the Molecular Magnetism, Dielectric Properties, new Emerging Technology Areas for Heterogeneous Integration, Polymer and Printed Electronics, advanced Bio-systems for Disposable Device, as well as gas sensor and multiscale modeling.

Giuseppe Milano is associate professor at the Department of Chemistry and Biology, University of Salerno. He got his degree in theoretical chemistry in 1995 and a Ph.D. in macromolecular chemistry. He has been guest scientist at Theory Group of Max Planck Institute for Polymer Research, in 2003 he has been Alexander Von Humboldt fellow at International University Bremen and in 2008 he was invited fellow of Japan Society for Promotion of Science at Tohoku University. His research interests are simulation methods in soft matter with particular interest devoted to development of methods for modeling polymeric materials across time and length scales.